NANO LETTERS

pubs.acs.org/NanoLett Letter

Breaking Anti-PT Symmetry by Spinning a Resonator

Huilai Zhang, Ran Huang, Sheng-Dian Zhang, Ying Li, Cheng-Wei Qiu, Franco Nori, and Hui Jing*

Cite This: https://dx.doi.org/10.1021/acs.nanolett.0c03119 Read Online

ACCESS | Metrics & More | Article Recommendations | Supporting Information

ABSTRACT: Non-Hermitian systems, with symmetric or antisymmetric Hamiltonians under the parity-time (PT) operations, can have entirely real or imaginary eigenvalues. This fact has led to surprising discoveries such as loss-induced lasing and topological energy transfer. A merit of anti-PT systems is free of gain, but in recent efforts on making anti-PT devices, nonlinearity is still required. Here, counterintuitively, we show how to achieve anti-PT symmetry and its spontaneous breaking in a linear device by spinning a lossy resonator. Compared with a Hermitian spinning device, significantly enhanced optical isolation and ultrasensitive nanoparticle sensing are achievable in the anti-PT-broken phase. In a broader view, our work provides a new tool to study anti-PT physics, with such a wide range of applications as anti-PT lasers, anti-PT gyroscopes, and anti-PT topological photonics or optomechanics.

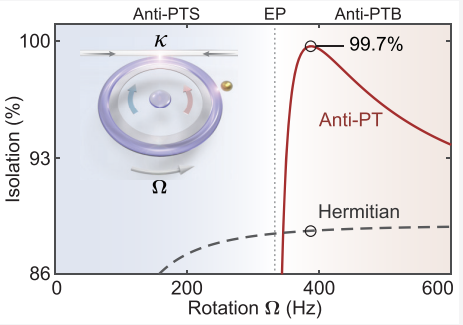

KEYWORDS: *non-Hermitian physics, anti-PT symmetry, spinning resonator, nonreciprocal light manipulation, nanoparticle sensing*

INTRODUCTION

Parity-time (PT) symmetry provides a way to relax the conventional Hermiticity condition to ensure real eigenvalues of quantum systems.[1,2] Particularly, by steering the system parameters to surpass or encircle the spectral degeneracy known as an exceptional point (EP),[3] striking differences emerge in the properties of PT devices. These differences, confirmed in diverse systems with the gain−loss balance,[4−19] have created opportunities to achieve exotic functionalities, such as loss-induced lasing or antilasing,[2,8,9] robust wireless power transfer,[16] and enhanced sensor responses[18−21] or light−matter interactions.[22−24]

A tremendous effort has also been witnessed in achieving anti-PT symmetry which does not need any gain,[25] thus providing a practical way to study quantum non-Hermitian effects.[26−28] Anti-PT symmetry has been demonstrated by using dissipatively coupled atomic beams,[29] and then by using cold atoms,[30] electrical circuits,[31] thermal materials,[32] and optical devices.[33−35] These breakthroughs have initiated the field of exploring unique anti-PT effects, e.g., energy-difference conserving dynamics[31] and chiral mode switching.[33]

Here, we show how to achieve and utilize optical anti-PT symmetry breaking by spinning a linear resonator.[36] We find that anti-PT symmetry emerging in such a device results in giant optical nonreciprocity and enhanced sensor performance. Our work is essentially different from the very recent work on anti-PT mode splitting in a nonlinear Brillouin device,[37] since (i) the momentum or phase matching condition, as required for Brillouin devices, is not needed here; (ii) the power condition, i.e., above a threshold to create the Brillouin scattering, although not strong enough to induce other nonlinearities, is also unnecessary here; in fact, for a spinning resonator, the input can be ranging from single photons to a high-power laser;[36] (iii) the spinning speed is much easier to be continuously tuned in situ than internal nonlinearity of materials. In a broader view, our work is well compatible with all the other well-established nonlinear or topological techniques, providing a feasible new way to engineer non-Hermitian devices, for applications in, for example, anti-PT metrology[38,39] and anti-PT topological photonics or nanomechanics.[33,40]

RESULTS AND DISCUSSIONS

Optical Anti-PT Symmetry. Anti-PT systems with two coupled modes can be described at the simplest level as[25,29]

$$H_{\mathrm{APT}} = \begin{pmatrix} \omega & \kappa \\ -\kappa^* & -\omega^* \end{pmatrix} \tag{1}$$

where ω is the complex frequency and κ is the complex coupling strength between the two optical modes. It indicates two conditions are required for realizing anti-PT symmetry: (i) two excited modes with opposite frequency detunings and same loss or gain; (ii) anti-Hermitian coupling between the modes. In previous experiments, optical anti-PT symmetry has been realized based on, for example, complex spatial structures[29,33] or nonlinear processes.[30,37]

As already demonstrated in the experiment,[38] see Figure 1a, we consider a linear optical resonator driven by two lasers with

Received: July 29, 2020
Revised: September 10, 2020

https://dx.doi.org/10.1021/acs.nanolett.0c03119
Nano Lett. XXXX, XXX, XXX−XXX

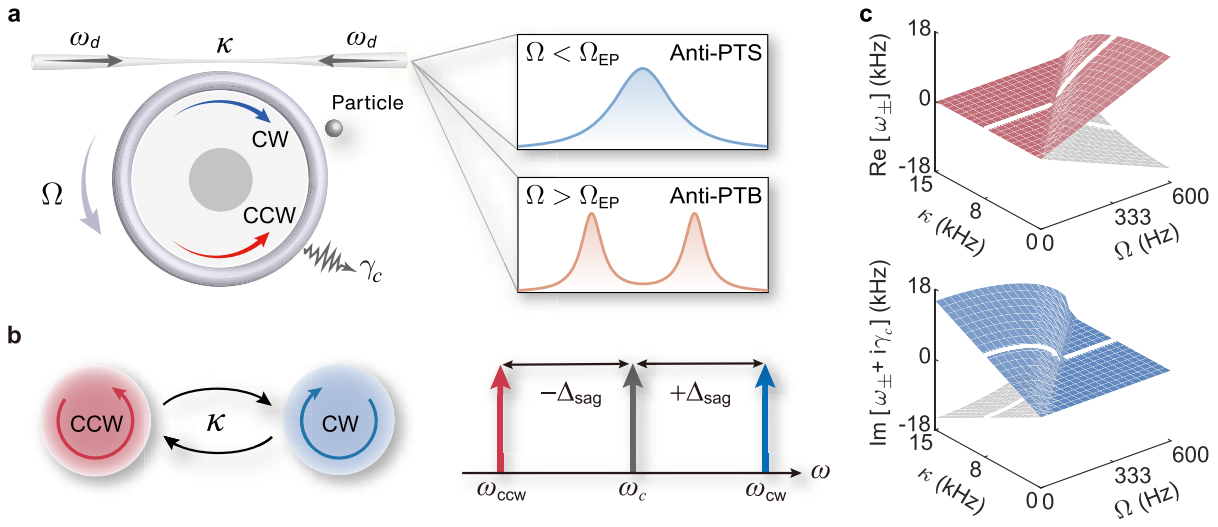

Figure 1. Anti-PT symmetry in a linear spinning resonator. (a) The resonator is driven by two lasers with the same frequency ω_d from the left and right. Anti-PT symmetry is realized with the opposite frequency shifts induced by the mechanical rotation with angular speed Ω and the dissipative coupling κ induced by the taper scattering. The output spectra in the anti-PT-symmetric (anti-PTS) and symmetry-broken (anti-PTB) phases can be observed by tuning Ω for $\Omega < \Omega_{EP}$ and $\Omega > \Omega_{EP}$, respectively, where Ω_{EP} is the angular speed at EP. The nanoparticle is to be measured. (b) The schematics of Sagnac effect and dissipative coupling show the physical mechanism of realizing anti-PT symmetry. (c) The real and imaginary parts of eigenfrequencies versus κ and Ω reveal the spectral properties of anti-PT symmetry. The white solid curves correspond to the case of $\kappa = 8$ kHz. For other parameter values, see the main text.

frequency ω_d from the left and right, which can excite the clockwise (CW) and counterclockwise (CCW) traveling modes. When the resonator is spinning at an angular velocity Ω,[36] the rotation-induced Sagnac–Fizeau shift $\omega_c \rightarrow \omega_c \pm \Delta_{sag}$ is given by[41]

$$\Delta_{sag} = \frac{nR\Omega\omega_c}{c}\left(1 - \frac{1}{n^2} - \frac{\lambda}{n}\frac{dn}{d\lambda}\right) \tag{2}$$

where ω_c is the resonant frequency of a nonspinning resonator, c (λ) is the speed (wavelength) of light, n and R are the refractive index and radius of the resonator, respectively. The dispersion term $dn/d\lambda$, characterizing the relativistic origin of the Sagnac effect, is relatively small in typical materials (~1%).[36] We fix the CCW rotation of the resonator; hence $+\Delta_{sag}(-\Delta_{sag})$ corresponds to the CW (CCW) traveling mode, see Figure 1b. The taper-scattering-induced dissipative backscattering leads to the dissipative coupling $i\kappa$ between the countercirculating modes,[38] which is anti-Hermitian, i.e., $-(i\kappa)^* = i\kappa$. Obviously, this Sagnac resonator naturally fulfills the conditions of the realization of anti-PT symmetry.

In a frame rotating at driving frequency ω_d, the effective Hamiltonian of this system is

$$H_0 = \begin{pmatrix} \Delta_+ - i\gamma_c & i\kappa \\ i\kappa & \Delta_- - i\gamma_c \end{pmatrix} \tag{3}$$

where $\Delta_\pm = \Delta_c \pm \Delta_{sag}$ are the optical detunings in the spinning case with the optical driving detuning $\Delta_c = \omega_c - \omega_d$, and $\gamma_c = (\gamma_0 + \gamma_{ex})/2$ is the total optical loss including the intrinsic loss of the resonator $\gamma_0 \equiv \omega_c/Q$ with the quality factor Q and the loss due to the coupling of the resonator with the fiber taper γ_{ex}. For $\Delta_c = 0$, anti-PT symmetry can be realized without any gain or nonlinearity, which is different from that using nonlinear Brillouin scattering to provide optical gain in a resonator.[37] Unlike PT symmetry, anti-PT symmetry is independent of the spatially separated gain–loss balanced structure.

The eigenfrequencies of this linear anti-PT-symmetric system are

$$\omega_\pm = -i\gamma_c \pm \sqrt{\Delta_{sag}^2 - \kappa^2} \tag{4}$$

indicating a phase transition as Ω varies. Figure 1c shows that, for small Ω ($\Delta_{sag} < \kappa$), the eigenmodes preserve anti-PT symmetry with the same resonance frequency but different line widths. The symmetry breaking occurs at EP ($\Delta_{sag} = \kappa$) where the eigenstates coalesce. For large Ω ($\Delta_{sag} > \kappa$), the system enters the symmetry-broken phase with bifurcating eigenmodes. For a specific dissipative coupling strength, e.g., $\kappa = 8$ kHz, the critical value of rotation speed is obtained as $\Omega_{EP} = 333$ Hz (see the white solid curves in Figure 1c).

Here, we take the experimentally accessible parameters:[42−44] $\lambda = 1550$ nm, $Q \approx 1 \times 10^{11}$, $\gamma_{ex} = \gamma_0/2$, $n = 1.44$, and $R = 50$ μm. As demonstrated in the experiment,[38] the dissipative coupling originating from taper scattering can be ~8 kHz. In a recent experiment,[36] light in a tapered fiber is evanescently coupled into or out of a linear resonator (mounted on a spinning turbine). The spinning can drag air into the coupling region, so that a boundary layer of air forms. Because of the air pressure, the taper lies at a height above the resonator, which can be several nanometers. If perturbation induces the taper to rise higher than the equilibrium, it floats back to its original position, a process called aerodynamical self-adjustment.[36] This process thus leads to a stable coupling between the fiber and the resonator, and the taper does not touch or stick to the spinning device even if the taper is pushed toward it.[36] This device is robust against the extra loss induced by the internal defects or other dissipative elements in practice. Also, as demonstrated in an experiment,[45] the Fizeau shift can be increased even for a slow rotary speed, by using a dispersion enhanced technique.[45]

Symmetry-Broken Nonreciprocity. When a probe light of frequency ω_p is incident from the left (right) side and using

https://dx.doi.org/10.1021/acs.nanolett.0c03119
Nano Lett. XXXX, XXX, XXX−XXX

the input-output relation (see the Supporting Information), the transmission rate T_{cw} (T_{ccw}) is

$$T_{cw,ccw} = \left| 1 + \frac{i\gamma_{ex}(\delta_p \mp \Delta_{sag})}{(\delta_p + \Delta_{sag})(\delta_p - \Delta_{sag}) + \kappa^2} \right|^2 \quad (5)$$

where $\delta_p = \Delta_p - i\gamma_c$, $\Delta_p = \omega_c - \omega_p$. Clearly, the term $\mp\Delta_{sag}$ is the origin of nonreciprocal light transmission. In the anti-PT-symmetric phase, $\Delta_{sag} < \kappa$, the difference of the two transmission rates is limited, while in the symmetry-broken phase, this difference becomes larger for $\Delta_{sag} > \kappa$, enabling better one-way transmission. To confirm this picture, we study the isolation of this anti-PT system, i.e., $I^{APT} = |T_{cw} - T_{ccw}|$, with normalized $T_{cw,ccw}$. Indeed, the symmetry-broken isolation is much larger than that in the symmetric phase, see Figure 2a, b.

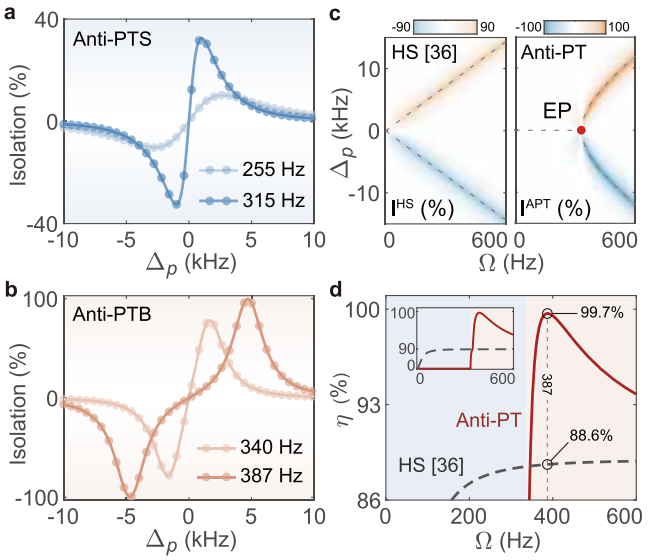

Figure 2. Nonreciprocal light transmission in the anti-PT-symmetric system. (a) Isolation I^{APT} versus probe detuning Δ_p with different rotation speed Ω in the anti-PT-symmetric phase and (b) symmetry-broken phase. (c) Isolations of Hermitian spinning (HS) resonator (left panel)[36] and anti-PT system (right panel) versus Ω and Δ_p. The gray dashed curves show the eigenfrequency evolutions of the two systems with respect to Ω. (d) Selected maximum isolation η as a function of Ω for anti-PT (red solid line) and HS (dark dashed line) systems. The other parameters are the same as those in Figure 1.

For a comparison, the optical isolation by using a Hermitian spinning (HS) resonator I^{HS}[36] and the selected maxima of the isolation $\eta \equiv \max[I]$ are also plotted in Figure 2c, d, respectively. The isolation of the HS system becomes larger by increasing Ω because of the optical mode splitting induced by the Sagnac shift but it is limited to 90% for the parameter values used here, because of the fixed line width.[36] In contrast, for an anti-PT device, both the line widths and the transmission can be altered, resulting in an enhanced isolation as high as 99.7%. This anti-PT-broken nonreciprocity, due to the interplay of synthetic angular momentum and dissipative backscattering, is fundamentally different from PT-symmetric nonreciprocity originating from nonlinearities.[6,7] One-way devices, free of exquisite control of gain or nonlinearity, have such a wide range of applications as on-chip circulator,[6,7] invisible sensing,[46,47] and quantum optical computation.[48]

Anti-PT sensor. In the presence of the external perturbation, the variation in the transmission spectrum also gives a way to detect the perturbation itself. For an example, taking into account a single nanoparticle falling into or flying by the evanescent field of the resonator,[49] see Figure 1a, we have the modified Hamiltonian of the perturbated system[49,50]

$$H_1 = \begin{pmatrix} \Delta'_+ - i\gamma_c + J & i\kappa + J \\ i\kappa + J & \Delta'_- - i\gamma_c + J \end{pmatrix} \quad (6)$$

where $\Delta'_\pm = \Delta_p \pm \Delta_{sag}$, and $J = g_1 - i\gamma_1$ is the complex perturbation induced by the nanoparticle with frequency shift g_1 and the line width broadening γ_1. As shown in Figure 3a, the eigenfrequency structure reveals how this system reacts on a sufficiently small perturbation. The sensitivity can be defined as the difference between the two eigenfrequencies:

$$\Delta\omega_1 = 2\sqrt{\Delta_{sag}^2 - (\kappa - iJ)^2} \quad (7)$$

Figure 3b, showing the logarithmic behavior of $\mathrm{Re}[\Delta\omega_1]$, highlights the sensitivity enhancement of the anti-PT sensor compared to that using an HS device.[36,49] For the same perturbation, the HS sensor performs closely to the anti-PT sensor when operating in the symmetry-broken phase. In the anti-PT-symmetric phase, the splitting is smaller than that in symmetry-broken phase. However, at EP, the slope of the response is 1/2, which can be explained by using perturbation theory. When J is much smaller than κ, the complex frequency splitting is expected to approximately follow

$$\Delta\omega_1 = 2\sqrt{2i\kappa}J^{1/2} \quad (8)$$

For larger J, the slope is slightly larger than 1/2 because in this case eq 7 cannot be simplified to eq 8 (see more details in the Supporting Information). In experiments,[20,50] the sensitivity defined by frequency splitting can be assessed by monitoring the separation of the spectral lines in transmission spectrum.

Sensitive responses to perturbations can also be revealed by measuring the variation of transmission spectrum.[49] Choosing, for example, the CW mode, the transmittance variation can be defined as $\mathcal{V}_s \equiv T_1^s/T_0^s$, where s denotes the anti-PT or HS sensor and $T_{1,0}^s$ is the transmission with or without the perturbation. Then we define the factor

$$\chi = \mathcal{V}_{APT}/\mathcal{V}_{HS} \quad (9)$$

to show the sensitivity enhancement of the anti-PT sensor. We find that by breaking the anti-PT symmetry, $\chi > 1$ can be achieved. In particular, for $\Omega \approx 386$ Hz, i.e., when the isolation reaches its maximum, 2 orders of magnitude enhanced sensitivity is achievable (see Figure 3c). This provides a conceptually new way to engineer an optical resonator to realize ultrasensitive nanoparticle sensors, as crucial elements in medical diagnosis and environmental monitoring.[52−54] In a broader view, by extending to a spinning nonlinear or optomechanical resonator, anti-PT devices can also be used to enhance the responses of, for example, gyroscopes or weak-force sensors.

In experiments,[51,53] nanoparticle sensing has been realized by measuring mode splitting. The particle falling through the mode volume of the resonator has a limited interaction time with the field, and, regardless of whether this time is very short or long, the resonator will feel and respond to it by exhibiting mode splitting.[55] A spinning resonator may induce the particle to diffuse in the air, which may change the overlap of the

https://dx.doi.org/10.1021/acs.nanolett.0c03119
Nano Lett. XXXX, XXX, XXX−XXX

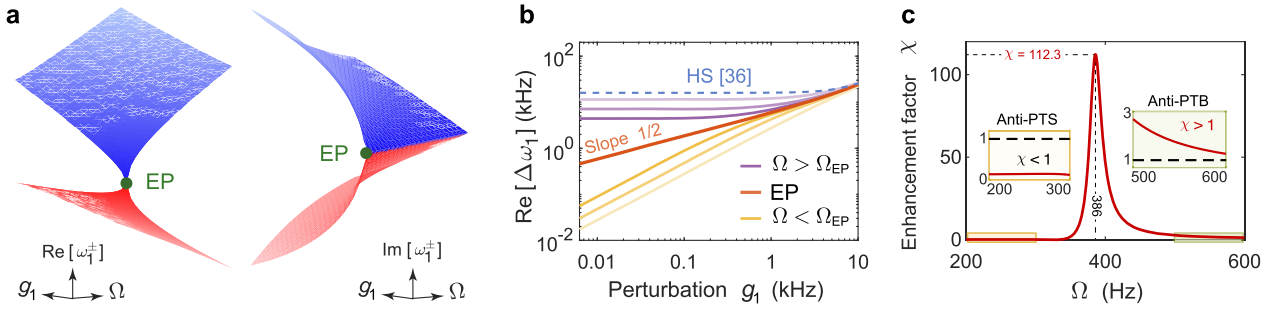

Figure 3. Anti-PT-symmetric ultrasensitive nanoparticle sensing. (a) The evolution of the eigenenergy of the perturbated system versus the perturbation g_1 induced by a single nanoparticle. Here we set $\gamma_1/g_1 = 0.05$ as that in the experiments.[50,51] (b) Dependence of frequency splitting Re $[\Delta\omega_1]$ corresponding to anti-PT sensor (solid curves) and HS sensor (dashed line)[36] on g_1. The yellow, purple and orange curves denote the cases in anti-PT-symmetric ($\Omega < \Omega_{EP}$) or symmetry-broken phase ($\Omega > \Omega_{EP}$), and at EP ($\Omega = \Omega_{EP}$), respectively. The rotation speed of HS sensor is chosen as $\Omega = \Omega_{EP} = 333$ Hz. (c) Enhancement factor χ as a function of Ω. Here, $g_1 = 3$ kHz and the probe detuning Δ_p is set to Re$[\omega_-]$. The other parameters are the same as those in Figure 1.

particle and the mode volume. The values of the frequency shift g_1 and the line width broadening γ_1 are thus changed by the particle position, but their ratio γ_1/g_1 remains unaffected (see the Supporting Information for details). Also, the particle position does not affect the Sagnac effect, and its detection in current experimental whispering-gallery-mode sensors can be very fast.[51,53] In the future, we will study more complicated cases such as the impact of time-varying coupling of the resonator and the flying-by nanoparticles and improved sensing efficiency by using, for example, the dispersion enhanced technique.[45]

CONCLUSIONS AND OUTLOOK

We have revealed anti-PT symmetry in a spinning resonator, without any optical nonlinearity or complex spatial structures. The opposite Sagnac frequency shifts and the optical dissipative coupling enable the system Hamiltonian to be antisymmetric under the combined PT operations. In particular, by breaking the anti-PT symmetry, enhanced optical nonreciprocity and nanoparticle sensing can be achieved in this linear device. Our work provides a highly feasible way to achieve anti-PT symmetry breaking and can be further extended to study nonlinear or higher order anti-PT effects by spinning a nonlinear device.[56]

Our scheme will not, of course, render other existing techniques obsolete. On the contrary, an anti-PT isolator can provide one-way light flow, whereas nonlinearity or synthetic dimensions can be integrated to induce or engineer nonlinear or quantum effects in anti-PT devices.[26,27] Our anti-PT resonator is thus well compatible with other well-developed techniques,[33,37] indicating exciting possibilities in non-Hermitian optics or nanomechanics.[24,57]

ASSOCIATED CONTENT

Supporting Information

The following files are available free of charge. The Supporting Information is available free of charge at https://pubs.acs.org/doi/10.1021/acs.nanolett.0c03119.

Experimental feasibility analysis and detailed derivations of the optical spectrum (PDF)

AUTHOR INFORMATION

Corresponding Author

Hui Jing − *Key Laboratory of Low-Dimensional Quantum Structures and Quantum Control of Ministry of Education, Department of Physics and Synergetic Innovation Center for Quantum Effects and Applications, Hunan Normal University, Changsha 410081, China;* orcid.org/0000-0001-5091-2057; Email: jinghui73@foxmail.com

Authors

Huilai Zhang − *Key Laboratory of Low-Dimensional Quantum Structures and Quantum Control of Ministry of Education, Department of Physics and Synergetic Innovation Center for Quantum Effects and Applications, Hunan Normal University, Changsha 410081, China;* orcid.org/0000-0002-3919-1655

Ran Huang − *Key Laboratory of Low-Dimensional Quantum Structures and Quantum Control of Ministry of Education, Department of Physics and Synergetic Innovation Center for Quantum Effects and Applications, Hunan Normal University, Changsha 410081, China;* orcid.org/0000-0003-3850-9403

Sheng-Dian Zhang − *Key Laboratory of Low-Dimensional Quantum Structures and Quantum Control of Ministry of Education, Department of Physics and Synergetic Innovation Center for Quantum Effects and Applications, Hunan Normal University, Changsha 410081, China;* orcid.org/0000-0002-6073-4263

Ying Li − *Interdisciplinary Center for Quantum Information, State Key Laboratory of Modern Optical Instrumentation, College of Information Science and Electronic Engineering and ZJU-Hangzhou Global Science and Technology Innovation Center, Key Lab. of Advanced Micro/Nano Electronic Devices & Smart Systems of Zhejiang, Zhejiang University, Hangzhou 310027, China;* orcid.org/0000-0002-2730-7171

Cheng-Wei Qiu − *Department of Electrical and Computer Engineering, National University of Singapore, Singapore 117583 Singapore;* orcid.org/0000-0002-6605-500X

Franco Nori − *Theoretical Quantum Physics Laboratory, RIKEN Cluster for Pioneering Research, Wako-shi, Saitama 351-0198, Japan; Physics Department, The University of Michigan, Ann Arbor, Michigan 48109-1040, United States;* orcid.org/0000-0003-3682-7432

Complete contact information is available at: https://pubs.acs.org/10.1021/acs.nanolett.0c03119

https://dx.doi.org/10.1021/acs.nanolett.0c03119
Nano Lett. XXXX, XXX, XXX−XXX

Notes

The authors declare no competing financial interest.

After the submission of our manuscript, a new paper was posted on arXiv, reporting experimental observations of anti-PT topology and anti-PT-enhanced Brillouin sensing in a fiber (with nonlinearity and gain).[58]

■ ACKNOWLEDGMENTS

We thank Li Ge at the City University of New York for his constructive suggestions. H.J. is supported by the National Natural Science Foundation of China under Grants 11935006 and 11774086. C.-W.Q. acknowledges the financial support from A*STAR Pharos Program (Grant 15270 00014, with Project R-263-000-B91-305) and Ministry of Education, Singapore (Project R-263-000-D11-114). F.N. is supported in part by NTT Research, Army Research Office (ARO) (Grant W911NF-18-1-0358), Japan Science and Technology Agency (JST) (via the Q-LEAP program and the CREST Grant JPMJCR1676), Japan Society for the Promotion of Science (JSPS) (via the KAKENHI Grant JP20H00134, and the JSPS-RFBR Grant JPJSBP120194828), and the Foundational Questions Institute Fund (FQXi) (Grant FQXi-IAF19-06), a donor-advised fund of the Silicon Valley Community Foundation.

■ REFERENCES

(1) Bender, C. M.; Boettcher, S. Real Spectra in Non-Hermitian Hamiltonians Having PT Symmetry. *Phys. Rev. Lett.* **1998**, *80*, 5243−5246.

(2) Özdemir, Ş. K.; Rotter, S.; Nori, F.; Yang, L. Parity−Time Symmetry and Exceptional Points in Photonics. *Nat. Mater.* **2019**, *18*, 783−798.

(3) Miri, M.-A.; Alù, A. Exceptional Points in Optics and Photonics. *Science* **2019**, *363*, No. eaar7709.

(4) Guo, A.; Salamo, G. J.; Duchesne, D.; Morandotti, R.; Volatier-Ravat, M.; Aimez, V.; Siviloglou, G. A.; Christodoulides, D. N. Observation of PT-Symmetry Breaking in Complex Optical Potentials. *Phys. Rev. Lett.* **2009**, *103*, No. 093902.

(5) Rüter, C. E.; Makris, K. G.; El-Ganainy, R.; Christodoulides, D. N.; Segev, M.; Kip, D. Observation of Parity-Time Symmetry in Optics. *Nat. Phys.* **2010**, *6*, 192−195.

(6) Chang, L.; Jiang, X.; Hua, S.; Yang, C.; Wen, J.; Jiang, L.; Li, G.; Wang, G.; Xiao, M. Parity-Time Symmetry and Variable Optical Isolation in Active-Passive-Coupled Microresonators. *Nat. Photonics* **2014**, *8*, 524−529.

(7) Peng, B.; Özdemir, Ş. K.; Lei, F.; Monifi, F.; Gianfreda, M.; Long, G. L.; Fan, S.; Nori, F.; Bender, C. M.; Yang, L. Parity-Time-Symmetric Whispering-Gallery Microcavities. *Nat. Phys.* **2014**, *10*, 394−398.

(8) Feng, L.; Wong, Z. J.; Ma, R.-M.; Wang, Y.; Zhang, X. Single-Mode Laser by Parity-Time Symmetry Breaking. *Science* **2014**, *346*, 972−975.

(9) Hodaei, H.; Miri, M.-A.; Heinrich, M.; Christodoulides, D. N.; Khajavikhan, M. Parity-Time-Symmetric Microring Lasers. *Science* **2014**, *346*, 975−978.

(10) Wimmer, M.; Regensburger, A.; Miri, M.-A.; Bersch, C.; Christodoulides, D. N.; Peschel, U. Observation of Optical Solitons in PT-Symmetric Lattices. *Nat. Commun.* **2015**, *6*, 7782.

(11) Li, J.; Harter, A. K.; Liu, J.; de Melo, L.; Joglekar, Y. N.; Luo, L. Observation of Parity-Time Symmetry Breaking Transitions in a Dissipative Floquet System of Ultracold Atoms. *Nat. Commun.* **2019**, *10*, 855.

(12) Zhu, X.; Ramezani, H.; Shi, C.; Zhu, J.; Zhang, X. PT -Symmetric Acoustics. *Phys. Rev. X* **2014**, *4*, No. 031042.

(13) Zhu, W.; Fang, X.; Li, D.; Sun, Y.; Li, Y.; Jing, Y.; Chen, H. Simultaneous Observation of a Topological Edge State and Exceptional Point in an Open and Non-Hermitian Acoustic System. *Phys. Rev. Lett.* **2018**, *121*, 124501.

(14) Schindler, J.; Li, A.; Zheng, M. C.; Ellis, F. M.; Kottos, T. Experimental Study of Active LRC Circuits with PT Symmetries. *Phys. Rev. A: At., Mol., Opt. Phys.* **2011**, *84*, No. 040101.

(15) Bittner, S.; Dietz, B.; Günther, U.; Harney, H. L.; Miski-Oglu, M.; Richter, A.; Schäfer, F. PT Symmetry and Spontaneous Symmetry Breaking in a Microwave Billiard. *Phys. Rev. Lett.* **2012**, *108*, No. 024101.

(16) Assawaworrarit, S.; Yu, X.; Fan, S. Robust Wireless Power Transfer Using a Nonlinear Parity−Time-Symmetric Circuit. *Nature (London, U. K.)* **2017**, *546*, 387−390.

(17) Lü, X.-Y.; Jing, H.; Ma, J.-Y.; Wu, Y. PT-Symmetry-Breaking Chaos in Optomechanics. *Phys. Rev. Lett.* **2015**, *114*, 253601.

(18) Chen, P.-Y.; Sakhdari, M.; Hajizadegan, M.; Cui, Q.; Cheng, M. M.-C.; El-Ganainy, R.; Alù, A. Generalized Parity−Time Symmetry Condition for Enhanced Sensor Telemetry. *Nat. Electron.* **2018**, *1*, 297−304.

(19) Dong, Z.; Li, Z.; Yang, F.; Qiu, C.-W.; Ho, J. S. Sensitive Readout of Implantable Microsensors Using a Wireless System Locked to an Exceptional Point. *Nat. Electron.* **2019**, *2*, 335−342.

(20) Hodaei, H.; Hassan, A. U.; Wittek, S.; Garcia-Gracia, H.; El-Ganainy, R.; Christodoulides, D. N.; Khajavikhan, M. Enhanced Sensitivity at Higher-Order Exceptional Points. *Nature (London, U. K.)* **2017**, *548*, 187−191.

(21) Xiao, Z.; Li, H.; Kottos, T.; Alù, A. Enhanced Sensing and Nondegraded Thermal Noise Performance Based on PT-Symmetric Electronic Circuits with a Sixth-Order Exceptional Point. *Phys. Rev. Lett.* **2019**, *123*, 213901.

(22) Jing, H.; Özdemir, S. K.; Lü, X.-Y.; Zhang, J.; Yang, L.; Nori, F. PT -Symmetric Phonon Laser. *Phys. Rev. Lett.* **2014**, *113*, No. 053604.

(23) Zhang, J.; Peng, B.; Özdemir, Ş. K.; Pichler, K.; Krimer, D. O.; Zhao, G.; Nori, F.; Liu, Y.-x.; Rotter, S.; Yang, L. A Phonon Laser Operating at an Exceptional Point. *Nat. Photonics* **2018**, *12*, 479−484.

(24) Xu, H.; Mason, D.; Jiang, L.; Harris, J. G. E. Topological Energy Transfer in an Optomechanical System with Exceptional Points. *Nature (London, U. K.)* **2016**, *537*, 80−83.

(25) Ge, L.; Türeci, H. E. Antisymmetric PT-Photonic Structures with Balanced Positive- and Negative-Index Materials. *Phys. Rev. A: At., Mol., Opt. Phys.* **2013**, *88*, No. 053810.

(26) Cao, W.; Lu, X.; Meng, X.; Sun, J.; Shen, H.; Xiao, Y. Reservoir-Mediated Quantum Correlations in Non-Hermitian Optical System. *Phys. Rev. Lett.* **2020**, *124*, No. 030401.

(27) Wu, Y.; Liu, W.; Geng, J.; Song, X.; Ye, X.; Duan, C.-K.; Rong, X.; Du, J. Observation of Parity-Time Symmetry Breaking in a Single-Spin System. *Science* **2019**, *364*, 878−880.

(28) Klauck, F.; Teuber, L.; Ornigotti, M.; Heinrich, M.; Scheel, S.; Szameit, A. Observation of PT-Symmetric Quantum Interference. *Nat. Photonics* **2019**, *13*, 883−887.

(29) Peng, P.; Cao, W.; Shen, C.; Qu, W.; Wen, J.; Jiang, L.; Xiao, Y. Anti-Parity-Time Symmetry with Flying Atoms. *Nat. Phys.* **2016**, *12*, 1139−1145.

(30) Jiang, Y.; Mei, Y.; Zuo, Y.; Zhai, Y.; Li, J.; Wen, J.; Du, S. Anti-Parity-Time Symmetric Optical Four-Wave Mixing in Cold Atoms. *Phys. Rev. Lett.* **2019**, *123*, 193604.

(31) Choi, Y.; Hahn, C.; Yoon, J. W.; Song, S. H. Observation of an Anti-PT-Symmetric Exceptional Point and Energy-Difference Conserving Dynamics in Electrical Circuit Resonators. *Nat. Commun.* **2018**, *9*, 2182.

(32) Li, Y.; Peng, Y.-G.; Han, L.; Miri, M.-A.; Li, W.; Xiao, M.; Zhu, X.-F.; Zhao, J.; Alù, A.; Fan, S.; Qiu, C.-W. Anti-Parity-Time Symmetry in Diffusive Systems. *Science* **2019**, *364*, 170−173.

(33) Zhang, X.-L.; Jiang, T.; Chan, C. T. Dynamically Encircling an Exceptional Point in Anti-Parity-Time Symmetric Systems: Asymmetric Mode Switching for Symmetry-Broken Modes. *Light: Sci. Appl.* **2019**, *8*, 88.

(34) Li, Q.; Zhang, C.-J.; Cheng, Z.-D.; Liu, W.-Z.; Wang, J.-F.; Yan, F.-F.; Lin, Z.-H.; Xiao, Y.; Sun, K.; Wang, Y.-T.; Tang, J.-S.; Xu, J.-S.;

https://dx.doi.org/10.1021/acs.nanolett.0c03119
Nano Lett. XXXX, XXX, XXX−XXX

Li, C.-F.; Guo, G.-C. Experimental Simulation of Anti-Parity-Time Symmetric Lorentz Dynamics. *Optica* **2019**, *6*, 67.
(35) Zhao, J.; Liu, Y.; Wu, L.; Duan, C.-K.; Liu, Y.-x.; Du, J. Observation of Anti-PT-Symmetry Phase Transition in the Magnon-Cavity-Magnon Coupled System. *Phys. Rev. Appl.* **2020**, *13*, No. 014053.
(36) Maayani, S.; Dahan, R.; Kligerman, Y.; Moses, E.; Hassan, A. U.; Jing, H.; Nori, F.; Christodoulides, D. N.; Carmon, T. Flying Couplers above Spinning Resonators Generate Irreversible Refraction. *Nature (London, U. K.)* **2018**, *558*, 569−572.
(37) Zhang, F.; Feng, Y.; Chen, X.; Ge, L.; Wan, W. Synthetic Anti-PT Symmetry in a Single Microcavity. *Phys. Rev. Lett.* **2020**, *124*, No. 053901.
(38) Lai, Y.-H.; Lu, Y.-K.; Suh, M.-G.; Yuan, Z.; Vahala, K. Observation of the Exceptional-Point-Enhanced Sagnac Effect. *Nature (London, U. K.)* **2019**, *576*, 65−69.
(39) Hokmabadi, M. P.; Schumer, A.; Christodoulides, D. N.; Khajavikhan, M. Non-Hermitian Ring Laser Gyroscopes with Enhanced Sagnac Sensitivity. *Nature (London, U. K.)* **2019**, *576*, 70−74.
(40) Lee, T. E.; Reiter, F.; Moiseyev, N. Entanglement and Spin Squeezing in Non-Hermitian Phase Transitions. *Phys. Rev. Lett.* **2014**, *113*, 250401.
(41) Malykin, G. B. The Sagnac Effect: Correct and Incorrect Explanations. *Phys.-Usp.* **2000**, *43*, 1229−1252.
(42) Armani, D. K.; Kippenberg, T. J.; Spillane, S. M.; Vahala, K. J. Ultra-High-Q Toroid Microcavity on a Chip. *Nature (London, U. K.)* **2003**, *421*, 925−928.
(43) Huet, V. Millisecond Photon Lifetime in a Slow-Light Microcavity. *Phys. Rev. Lett.* **2016**, *116*, 133902.
(44) Peng, B.; Ozdemir, S. K.; Rotter, S.; Yilmaz, H.; Liertzer, M.; Monifi, F.; Bender, C. M.; Nori, F.; Yang, L. Loss-Induced Suppression and Revival of Lasing. *Science* **2014**, *346*, 328−332.
(45) Qin, T.; Yang, J.; Zhang, F.; Chen, Y.; Shen, D.; Liu, W.; Chen, L.; Jiang, X.; Chen, X.; Wan, W. Fast- and Slow-Light-Enhanced Light Drag in a Moving Microcavity. *Commun. Phys.* **2020**, *3*, 118.
(46) Fleury, R.; Sounas, D.; Alù, A. An Invisible Acoustic Sensor Based on Parity-Time Symmetry. *Nat. Commun.* **2015**, *6*, 5905.
(47) Cai, W.; Chettiar, U. K.; Kildishev, A. V.; Shalaev, V. M. Optical Cloaking with Metamaterials. *Nat. Photonics* **2007**, *1*, 224−227.
(48) Knill, E.; Laflamme, R.; Milburn, G. J. A Scheme for Efficient Quantum Computation with Linear Optics. *Nature* **2001**, *409*, 46−52.
(49) Jing, H.; Lü, H.; Özdemir, S. K.; Carmon, T.; Nori, F. Nanoparticle Sensing with a Spinning Resonator. *Optica* **2018**, *5*, 1424.
(50) Chen, W.; Kaya Ozdemir, S.; Zhao, G.; Wiersig, J.; Yang, L. Exceptional Points Enhance Sensing in an Optical Microcavity. *Nature (London, U. K.)* **2017**, *548*, 192−196.
(51) Peng, B.; Özdemir, Ş. K.; Liertzer, M.; Chen, W.; Kramer, J.; Yılmaz, H.; Wiersig, J.; Rotter, S.; Yang, L. Chiral Modes and Directional Lasing at Exceptional Points. *Proc. Natl. Acad. Sci. U. S. A.* **2016**, *113*, 6845−6850.
(52) Vollmer, F.; Arnold, S.; Keng, D. Single Virus Detection from the Reactive Shift of a Whispering-Gallery Mode. *Proc. Natl. Acad. Sci. U. S. A.* **2008**, *105*, 20701−20704.
(53) Zhu, J.; Ozdemir, S. K.; Xiao, Y.-F.; Li, L.; He, L.; Chen, D.-R.; Yang, L. On-Chip Single Nanoparticle Detection and Sizing by Mode Splitting in an Ultrahigh-Q Microresonator. *Nat. Photonics* **2010**, *4*, 46−49.
(54) Chen, P.; Tran, N. T.; Wen, X.; Xiong, Q.; Liedberg, B. Inflection Point of the Localized Surface Plasmon Resonance Peak: A General Method to Improve the Sensitivity. *ACS Sens.* **2017**, *2*, 235−242.
(55) Zhu, J.; Özdemir, Ş. K.; He, L.; Yang, L. Controlled Manipulation of Mode Splitting in an Optical Microcavity by Two Rayleigh Scatterers. *Opt. Express* **2010**, *18*, 23535−23543.
(56) Cao, P.; Li, Y.; Peng, Y.; Qiu, C.; Zhu, X. High-Order Exceptional Points in Diffusive Systems: Robust APT Symmetry against Perturbation and Phase Oscillation at APT Symmetry Breaking. *ES Energy Environ.* **2020**, *7*, 48−55.
(57) Yuan, L.; Lin, Q.; Xiao, M.; Fan, S. Synthetic Dimension in Photonics. *Optica* **2018**, *5*, 1396−1405.
(58) Bergman, A.; Duggan, R.; Sharma, K.; Tur, M.; Zadok, A.; Alu, A.Observation of Anti-Parity-Time-Symmetry, Phase Transitions and Exceptional Points in an Optical Fibre. *arXiv (Physics.Optics*, 2020, 2008.03126. https://arxiv.org/abs/2008.03126 (accessed 2020-08-07).

https://dx.doi.org/10.1021/acs.nanolett.0c03119
Nano Lett. XXXX, XXX, XXX−XXX